



Automatic detection of active fires and burnt areas in forest areas using optical satellite imagery and deep learning methods

Yasin Demirel^{1,2} , Tarık Türk ^{*2} 

¹Bartın University, Department of Information Technology, Bartın, Türkiye

²Sivas Cumhuriyet University, Faculty of Engineering, Department of Geomatics Engineering, 58140, Sivas, Türkiye

Cite this study:

Demirel, Y., & Türk, N. (2024). Automatic detection of active fires and burnt areas in forest areas using optical satellite imagery and deep learning methods. *Mersin Photogrammetry Journal*, 6 (2), 66-78.

<https://doi.org/10.53093/mephoj.1575877>

Keywords

Deep Learning
Active Fire Detection
Burnt Area Detection
CNN
Artificial Intelligence

Research/Review Article

Received:30.10.2024
Revised: 28.11.2024
Accepted:28.11.2024
Published:31.12.2024



Abstract

Forest fires have important ecological, social and economic consequences causing loss of life and property. In order to prevent these consequences, it is very important to intervene in active fires in a timely manner and to determine the extent of burnt areas as soon as possible. In such studies, remote sensing methods provide great benefits in terms of speed and cost. In recent years, various methods have been developed to segment active fires and burnt areas with satellite images. Deep learning methods successfully perform segmentation processes in many areas such as disease detection in the field of health, crop type determination in the field of agriculture, land use and building detection in the field of urbanization. In this study, a method has been developed that automatically detects both active fires and burned areas that need to be re-enacted in terms of location and area size by using the same Sentinel 2 scene in a single time using deep learning methods. In particular, a new training and validation data set was created to train the U-Net+InceptionResNetV2 (CNN) model. By combining the powerful features of U-Net with InceptionResNet V2, a convolutional neural network trained over more than one million images on the ImageNet very base, we aim to examine its capabilities in burned area and active fire detection. The model applied on the test data has been shown to give successful results with an overall accuracy of 0.97 and an IoU (Intersection over union) value of 0.88 in the detection of burnt areas, and an overall accuracy of 0.99 and an IoU value of 0.82 in the detection of active fires. Finally, when the test images that were not used in the training dataset were evaluated with the trained model, it was revealed that the results were quite consistent in the detection of active fires and burnt areas and their geographical locations.

1. Introduction

Forests cover one third of the world's terrestrial areas. They are of vital importance for all living things due to factors such as ensuring natural balance, sustainability of ecosystem activities, regulation of water resources and nutrient cycling (1, 2, 3). In addition, forests are one of the most important assets for our world in terms of biodiversity and climate, carbon storage functions against the greenhouse gas effect, and their role in creating a barrier against flood and erosion hazards (2, 4). Forest fires that destroy these unique assets lead to the decline of forest stands, impair forest health and biodiversity, and emit aerosols and other greenhouse gases that have impacts on the global carbon content (3).

The most important reason for the easy onset and rapid spread of forest fires can be shown as global climate change and the resulting global warming. Especially in the last century, greenhouse gases emitted during activities such as agriculture, industry, animal husbandry and logistics have been the main cause of climate change. The Mediterranean climate, which is hot and dry in summer, increases the risk of fire and causes fires to occur in large areas and for a long time (1, 2). In recent years, the world has been exposed to many forest fire disasters caused by factors such as negligence, accident and intention (1). Türkiye is covered with approximately 23 million hectares of forest area. While the total number of fires of 500 hectares or more, which are considered as large fires in Türkiye, is 25 in the last ten years, Türkiye has been exposed to 16 large fires only in 2021. Factors such as negligence, accident and

intention cause forest fires. The Intergovernmental Panel on Climate Change (IPCC) has revealed that the global temperature, which has increased by 1.2 C° since the pre-industrial period, has caused an increasing number of droughts and forest fires (1, 3). Forest fires, which are a critical and global event, are exacerbated by climate change and cause significant economic and environmental damage annually (4).

It is crucial to obtain information on the location, extent and frequency of fire events in order to coordinate emergency responses on the ground, identify economic and ecological losses, and assess the recovery process. Compared to terrestrial methods, remote sensing data are highly advantageous in terms of time and cost (2, 3, 4). Recently, due to the reasons mentioned above, forest fires have become one of the topics of great interest in the scientific world.

Optical sensors are widely preferred for analyzing active fires and burnt areas. This is because burning biomass must have clear effects to be detected. In contrast, radar sensors are less favoured than optical imagery in such studies due to the opposite effects of radar measurements on the backscattering coefficient during the burning of biomass (3). However, there are also some common problems with optical imagery when identifying burned areas. First of all, there is the problem of atmospheric opacity. The presence of fire smoke and clouds prevents the observation of burned areas, and even cloud shadows can cause false detections (5). In addition, sensor characteristics are also an important detail in the detection of fires. It has been observed that low-resolution sensors are insufficient especially in the detection of small and fragmented burnt areas (6). On the other hand, if burnt areas do not cover a complete pixel area, these areas may co-locate spectrally and spatially with different land plant species (7). High resolution sensors reduce this problem considerably. In other words, the general problem when working with coarse resolution data is that small and fragmented active fires and small and fragmented burnt areas caused by fires cannot be detected. Therefore, this situation negatively affects the segmentation results (3, 4). For this reason, products have been developed for the use of higher resolution images. Sentinel 2 optical satellite imagery, which has been freely available since 2015, represents a good balance between temporal and spatial resolution. The images have a temporal resolution of five days and a spatial resolution ranging from 10 m to 60 m (3). In addition, Sentinel 2 satellite imagery is widely used in studies on mapping burned areas and determining active fires in the literature (3, 4, 8, 9, 10).

Many studies have been carried out in the literature on the detection of active forest fires and mapping of burnt areas. The current and important ones of these studies are taken into consideration and analyzed.

Kavzoğlu et al. (11) aimed to analyze the forest fires that occurred in Manavgat, Marmaris and Bodrum districts in July and August 2021 using remote sensing techniques and multi-temporal satellite images and to determine the boundaries of the damaged areas. Using Sentinel 2 satellite imagery before, during and after the fire, burn severity difference maps were produced and

Normalized Difference Vegetation Index (NDVI) was calculated to evaluate the burn severity levels both visually and metrically during and after the fire periods. The performance of spectral indices such as Middle Infrared Burn Index (MIRBI), Burned Area Index (BAI), Normalized Burn Ratio (NBR), Char Soil Index (CSI) in separating burned areas from unburned areas was evaluated.

Musaoğlu et al. (12) emphasized the importance of accurate information production and up-to-date information in forest fire preparedness. In this context, the importance of GIS together with remote sensing data in determining fire vulnerability and risk analysis with up-to-date data was mentioned.

De Almeida Pereira et al. (13) studied how different convolutional neural network architectures can be used in active fire detection studies with Landsat 8 satellite images and compared the performance of the models trained on automatically segmented image patches with the original algorithm.

Seydi et al. (14) detected fires with the help of Landsat 8 satellite images. After applying some pre-processing steps such as radiometric correction and orthorectification to Landsat 8 satellite images, atmospheric correction was performed with the Fast Line of Sight Atmospheric Analysis of Hypercubes (FLAASH) module. The Fire-Net Architecture created in this study is compared with other common machine learning algorithms and its performance is evaluated.

In the study by Boothman and Cardille (15), low spatial, temporal and spectral resolution satellite images obtained from Landsat Multispectral Scanner (MSS) platform before 1980 were trained on U-Net architecture using deep learning methods and burnt area analysis was performed.

Khryashchev and Larionav (16), presented a convolutional neural network for automatic burnt area detection on high-resolution aerial images. Satellite images with different resolutions were also used to train and test this neural network. In the study, the images were analysed with the U-ResNet34 model, which was created by combining ResNet34 and U-Net neural networks as encoders.

In the study by Knopp et al. (3), segmentation of burnt areas was performed as a result of training the dataset created using NIR and SWIR bands of Sentinel 2 satellite images using U-Net architecture within the deep learning framework.

In the study by Zhang et al. (4), data collection and pre-processing, deep learning-based active fire detection and final product creation processes were performed using SWIR, NIR and Red bands of Sentinel 2 satellite images. In the study, the performances of DeepLabV3, HRNetV2 and DCPA+HRNetV2 models were evaluated.

Atasever and Tercan (17) used the Stacked Autocoders method based on deep learning for mapping burned forest areas from Sentinel-2 satellite images. This unsupervised learning method was combined with frequently used supervised learning algorithms (k-Nearest Neighbors, Subspace k-NN, Support Vector Machines, Random Forest, Bagged Decision Tree, Naive Bayes and Linear Discriminant Analysis) in two different

burned forest regions. both qualitatively and quantitatively. The study aims to provide an objective assessment by selecting regions with different structural characteristics. For the accuracy assessment, manually digitized burned areas from Sentinel-2 images were used. Different classification performance and quality metrics (Overall Accuracy, Mean Squared Error, Correlation Coefficient, Structural Similarity Index Measure, Peak Signal-to-Noise Ratio, Universal Image Quality Index and KAPPA metrics) were used for comparison. Furthermore, the consistency of the Stacked Autocoders method is analyzed with box plots. The results show that the Stacked Autocoders method has the highest accuracy values in both quantitative and qualitative analysis.

Fusioka et al. (18) addressed active fire segmentation in satellite imagery, a remote sensing task that is critical for planning, decision making and policy development. Although robust algorithms have been developed for this purpose for some satellites such as MODIS and Landsat-8, there is still a lack of an effective solution for important satellites such as Sentinel-2. To fill this gap, researchers have attempted to train convolutional and transformer-based deep learning architectures (U-Net, DeepLabV3+ and SegFormer) for active fire segmentation using transfer learning. They pre-trained their model with Landsat-8 images and automatically labeled samples and then fine-tuned it on Sentinel-2 images. Experimental results show that the proposed method achieves F1 scores of up to 88.4% on Sentinel-2 data, outperforming the three threshold-based algorithms by at least 19%.

Classification algorithms for forest fire segmentation can be divided into rule-based and machine learning approaches. Rule-based approaches detect spectral changes in the NIR and SWIR bands of Sentinel satellite imagery relative to the surroundings of burned areas and define thresholds for spectral bands or spectral indices (3). Similarly, active fires are detected by filtering high-value pixels in the B12 and B11 bands of Sentinel satellite images and low-value pixels in the B4 band (4). The indices commonly used in the literature for burned area segmentation are the Normalized Burn Ratio Index (NBR) (19), The Middle Infrared Burn Index (MIRBI) (20) and the Modified Burned Area Index (BAIM) (21). In general, in studies conducted without using machine learning and deep learning algorithms, not only post-fire images but also pre-fire images are needed. The working logic of this is to calculate spectral indices for the pre-event and post-event images and detect changes in pixels. The disadvantage of this is that the use of inadequate pre-event images exposed to cloud and glare effects may lead to misclassification. Unlike rule-based approaches, in machine learning approaches, active fires and burnt areas are learnt from a set of labelled data. Examples of Machine Learning algorithms are Support Vector Machines (SVM) (22) and Random Forest (RF) (23, 24).

Another machine learning field frequently preferred in remote sensing is convolutional neural networks (CNN), which we call deep learning. CNN connects only neurons within a receptive field (neighborhood), not all

neurons of consecutive layers, and reduces the computational time required by allowing contextual information to be integrated. Furthermore, the deep layer architecture enables the network to map any non-linear function and generalize the learned features. Here, the multiple layers in the network are the reason why CNNs are often referred to as deep learning architectures (3). CNNs can be used in many sensitive studies such as the detection of diseases in the field of health (25, 26), buildings (27), clouds (28), slums (29), water (30), land use (31), crop types (32) and human privacy (33). On the other hand, machine learning algorithms such as SVM and RF require extensive input data and need auxiliary data. On the other hand, deep learning algorithms in the form of CNNs can perform segmentation by generalizing features through labelled data without the need for any auxiliary data. For this reason, deep learning-based CNN architectures have been very promising in studies such as active fire detection and burned area mapping.

Compared to Landsat satellite imagery, which is frequently used in studies on forest fires, Sentinel 2 satellite imagery has better temporal resolution. Therefore, the possibility of obtaining cloud-free data at more frequent visit intervals increases even more. The biggest challenge in building a neural network model for active fire and burned area detection is the availability of training data containing spatial information. In order to increase the impact of training data on the performance of the network, it is necessary to determine the optimal band combinations for active forest fires and burned area detection separately (3,4).

Considering the above-mentioned studies, it is extremely important to introduce a method that performs data acquisition, data pre-processing, burnt area and active fire segmentation model, current location information of active fires and burnt areas, and calculation of active fire and burnt area sizes fully automatically in emergency response to forest fires and taking necessary measures as well as rehabilitation of burnt areas. Within the scope of this study, a software has been developed to automatically detect actively burning, burned and unburned areas using different band combinations of the same image by training Sentinel 2 satellite images, which are freely available for free use, with U-Net+Inception ResNetV2 deep learning architecture that can use the powerful features of U-Net and InceptionResNet V2 models trained with more than a million data, and to automatically perform geographical and metric analysis with Python programming language. Thus, with this study, if the date and location information of the image obtained from Sentinel 2 satellite on any date is defined to the software, active fire areas and burnt areas can be determined automatically.

2. Material and Method

2.1. Data

The most important feature that distinguishes deep learning algorithms from machine learning is that they require hardware with very high computational power in relation to their complex structure and large data size (34). In relation to this, in deep learning-based image

processing studies, a large number of labelled data is required while training the model.

In active fire area segmentation, pixels with active fire and pixels without active fire are manually labeled, similarly in burned area segmentation, burned pixels and unburned pixels are manually labeled and the data set is prepared. In this study, Sentinel 2 imagery was preferred as it is considered to be more useful than other free satellite imagery in terms of spatial and temporal resolution. Sentinel 2 satellite imagery covers 13 spectral bands, each with a spatial resolution between 10 and 60 m (Table 1).

A data search was conducted by considering fires in different locations around the world, such as Algeria, different states of the United States and Türkiye. A new dataset was compiled for training, validation and testing by considering images with appropriate features. In this direction, an atmospheric correction code was written in Python programming language using the Earth Engine library provided by Google using the metadata in the satellite images to use the images of the fire dates observed by the Sentinel 2 satellite. Then, the dates and locations from which the data were to be obtained were defined in the software. A buffer zone was created

around 58 km of the defined locations and all Sentinel 2 scenes for that date within the buffer zone were automatically determined by the software. SWIR1, SWIR2 and Red band combinations (Figure 1.b) were determined for the detection of active fires and SWIR2, NIR and Blue band combinations (Figure 1.a) were determined for burnt area detection. In Sentinel 2 images, the burned area causes a strong decrease in the near infrared (NIR) band (B8) and the resulting drought causes a moderate increase in the Short-Wave Infrared (SWIR) band (B12) (3, 6). Similarly, active fire detection using Sentinel 2 data can be performed by filtering out high-value pixels in the SWIR bands (B12 and B11) and low-value pixels in the B4 band (4). The bands recommended in the literature were also visually analyzed and it was concluded that their use was sufficient. All selected bands were resampled to 20 m spatial resolution and fully automatic downloading was completed. Labelled masks were generated from the downloaded images. The images and masks were divided into 256x256 image patches using Python programming language in order to make it easier for the artificial intelligence to learn and to lighten the computational load.

Table 1. Spectral band characteristics of the Sentinel 2 satellite (adapted from 3)

Band	Description	Central Wavelength [nm]	Bandwidth [nm]	Spatial resolution [m]
B1	Aerosol	443	20	60
B2	Blue	490	65	10
B3	Green	560	35	10
B4	Red	665	30	10
B5	Vegetation edge	705	15	20
B6	Vegetation edge	740	15	20
B7	Vegetation edge	783	220	20
B8	NIR	842	115	10
B8a	Narrow NIR	865	20	20
B9	Water vapor	945	20	60
B10	Cirrus	1380	30	60
B11	SWIR1	1610	90	20
B12	SWIR2	2190	180	20

A total of 988 image patches for active fires and 2304 image patches for burnt areas were created by visual analysis of the appropriate data. The data set was split into approximately 80% training, 10% validation and 10% test sets. In order to increase the analysis capabilities against different images, each training tile was increased approximately three times by applying a series of random shifts, scales, rotations, reflections, etc. from data augmentation techniques on the training data. Data augmentation, rotation in the factor range [-30, 30], shift in both width and height in the factor range [-0.3, 0.3], shear transformation in the factor range [-0.5, 0.5], random zoom in the factor range [-0.3, 0.3], and both vertical and horizontal mirroring were performed by testing their suitability after visual analysis. Border reflection and nearest neighbour interpolation were used to bring the enlarged tiles back to the required 256x256 pixel segment size. The purpose of applying data augmentation in the study is to improve training by artificially creating more balanced classes and examples with a wider variety in the training dataset. In other words, the training data must be of sufficient variety and

size; both requirements can be met with data augmentation techniques. Studies (32, 34, 35, 36, 37) have shown that the application of data augmentation methods improves the accuracy of the results by 4-8% (39). A dataset consisting of 2368 patches for active fires and 5520 patches for burnt area was generated by applying the data augmentation processes mentioned above.

2.2 Realisation of fully automated data processing

Fully automatic active fire and burnt area analysis is shown in the workflow diagram in Figure 2.

The process chain (Figure 2) is implemented in Python using the Keras library within the deep learning framework. Keras is a deep learning library running on Tensorflow (42).

The main components realized within the scope of this study are described in detail below. In order to start the fully automated processing chain in the software developed using the Python programming language, the location to be studied and a time when the Sentinel 2

satellite is receiving data must be defined. Level L1C data are downloaded with radiometric calibration settings and orthorectification, but not atmospherically corrected (3). The data are downloaded through the ESA Copernicus Open Access Centre (43) using the developed programming interface (API). Before downloading the data, atmospheric corrections are made and all bands of the two band combinations to be used (BC1: B12, B11, B4 and BC2: B12, B8, B2) are resampled to 20 m spatial resolution. The downloaded BC1 band combinations are used to produce labels for active fire areas and the BC2 combinations are used to produce labels for burnt areas.

Downloaded images and generated masks are divided into 256x256 patches for training. All these data are trained in a CNN architecture with the software created and a product that detects active fire and burnt areas is created.

When any date and location information from Sentinel 2 satellite image acquisition is defined to the software, burnt area and active fire areas can be detected automatically. In addition to obtaining the location information of active fire areas and burnt areas from the result image generated by the software, the dimensions of the relevant areas can also be calculated automatically.

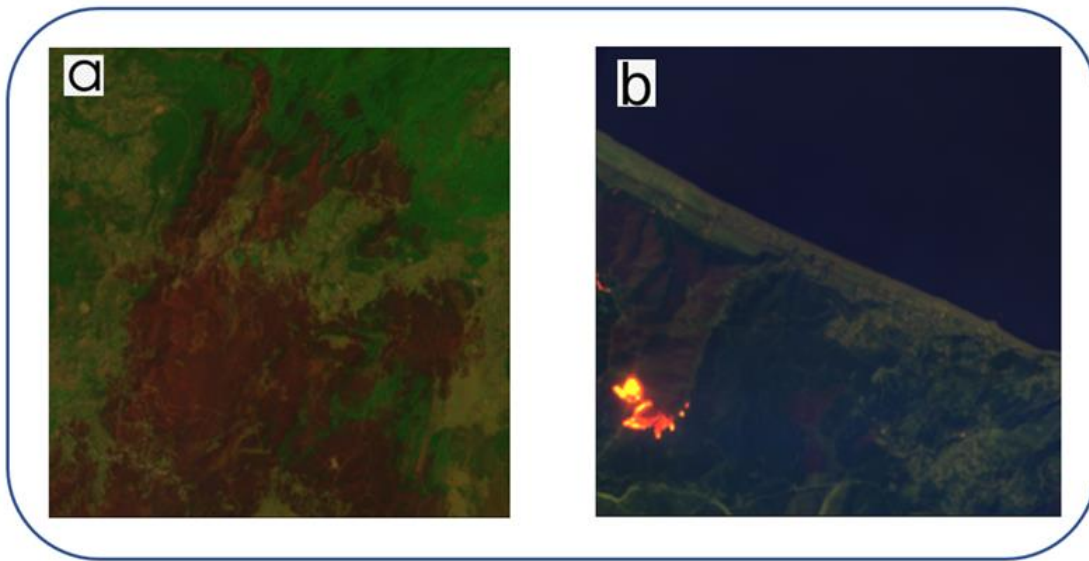


Figure 1. a) BC2: Image with B12, B8 and B2 band combination, b) BC1: Image with B12, B11 and B4 band combination

2.3 Semantic segmentation of fire areas with convolutional neural network

The most important part of this study is the development of a deep learning model based on CNN for segmentation. A neural network is a system of interconnected neurons used to model a complex function using many labelled data. A defined set of weights serves to complete the function. The neurons are organized as multiple cascaded layers allowing features to be learned in a hierarchical manner. During training, input tiles are propagated through the network and a loss function is calculated for quality assessment. The gradients of the loss functions are then propagated back through the network and the weights are adjusted accordingly to minimize the loss (3).

A critical point affecting the performance of the network is the network architecture. In this study, the U-Net model (Figure 3), which has been widely used in recent years and has proven its success, is preferred. The U-Net architecture was originally designed for biomedical image segmentation, but it has been shown to give good results in segmentation studies with satellite images such as cloud/cloud shadow and water segmentation (3). The U-Net architecture takes its name from its architecture similar to the letter U as shown in Figure 3.

U-Net is an architecture consisting of encoder and decoder convolutional neural network layers. The convolutional layers are trained iteratively and feature extraction is performed using the filters in these layers to learn features. The working principle of the U-Net architecture is to encode the image passing through the CNN in the encoder and then decode it in the decoder to obtain the segmentation mask. The attributes of the segmentation mask depend on the learnt weighting filters, the encoder and decoder networks, and the hopping and merging links.

In the encoder part, the input data is passed through five convolutional blocks where features are extracted at different scales. Each convolution block consists of two 3x3 convolutions with ReLU activation. Each one follows a batch normalization of the activations of the previous layer and the maximum pooling process ends with step 2, which samples the feature maps. The size of the feature maps is reduced by a factor 4 after each convolution block, while the number of feature channels is doubled. In the decoder part, the feature maps are also upsampled to the original image size by passing them through five blocks. Each of these blocks consists of a 2x2 transposed convolution which halves the number of feature channels, a concatenation with the corresponding feature map from the encoder part, and two 3x3 convolutions with ReLU activation, each followed by batch normalization. The last layer is a 1x1 convolution

with sigmoid activation to calculate the burn-in probability of each pixel (Figure 3).

The backbone is an architectural element that defines how these layers are organized in the encoder network and determines how the decoder network should be constructed. The backbones used are generally CNNs such as Inception, ResNet, VGG, EfficientNet, etc., which contain their own encoder and down-sampling. In this study, U-Net+InceptionResNetV2 backbone model is used for the segmentation algorithm.

InceptionResNetV2 (Figure 4) is a convolutional neural network trained on over one million images from the ImageNet database. The network is 164 layers deep and has categorised the images into 1000 object categories such as mouse, keyboard, pencil and many animals. As a result, the InceptionresNetV2 network is trained on rich feature representations for a wide variety of images. The network has an input image size of 299x299 and the output is a list of estimated class probabilities. It is formulated based on a combination of Inception structure and residual connectivity. In the InceptionResNet block, multidimensional convolutional filters are combined with residual links. The use of residual links eliminates the distortion problem caused by deep structures and also reduces the training time (44). The network architecture of InceptionResNetV2 is shown in Figure 4.

The U-Net+InceptionResNetV2 network was also trained on data sets such as shift scale and rotation. Thus, different geometric transformations can be used to process spatially resolved data.

In order to optimise the model, the loss function dice loss was used. Dice loss is a loss function used especially in processes such as image segmentation. This loss function is used to evaluate the performance of the model by measuring the similarity between the predicted segmentation map and the actual segmentation map (Equation 1).

$$Dice\ Loss = 1 - \frac{2|X \cap Y|}{|X| + |Y|} \quad (1)$$

Where X represents the estimated mask and Y represents the ground truth.

The learning rate was 0.0001 and the Adam optimization algorithm was used. The Adam optimization algorithm is advantageous for efficient Stochastic optimization requiring only first order gradients with low memory requirements. This optimization method calculates individual adaptive learning rates for different parameters from estimates of

the first and second moments of the gradients. The advantages of the Adam optimizer are that the magnitudes of the parameter updates are invariant in rescaling the gradient, the step sizes are approximately bounded by the step size hyperparameter, it does not require a stationary objective, and it works with sparse gradients (45). Validation data were also passed through the network during training, loss was calculated and monitored. At the end of the training process, the model associated with the lowest validation loss was saved. The Colab platform provided by Google was used in the model training. The workstation made available includes Intel(R) Xeon(R) CPU @ 2.00GHz, 8 cores, 64 GB RAM and Tesla T4 GPU unit.

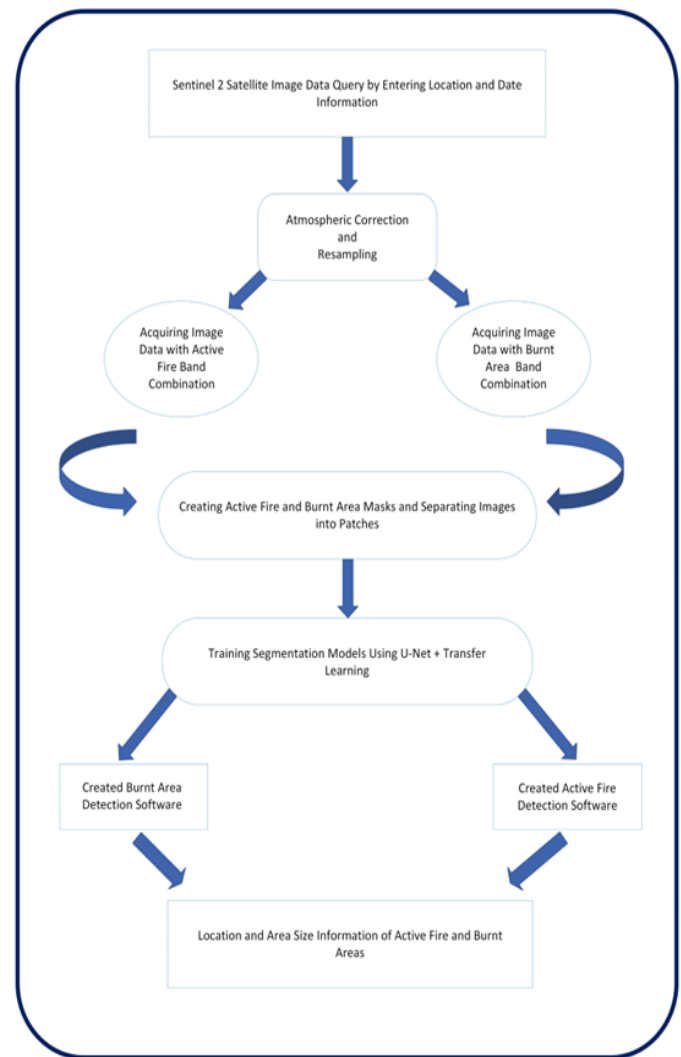


Figure 2. Workflow diagram

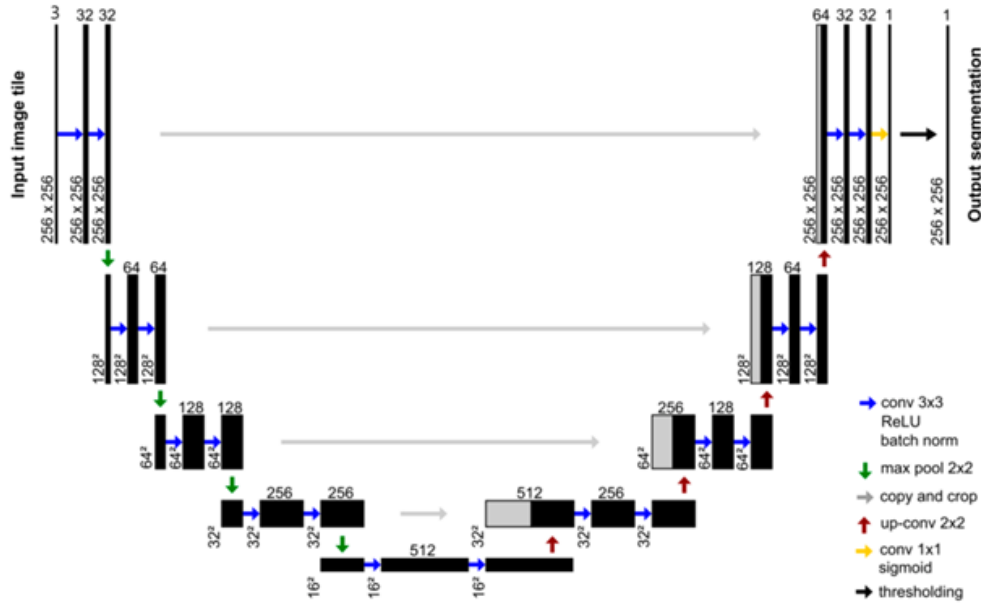


Figure 3. U-Net architecture used in the study

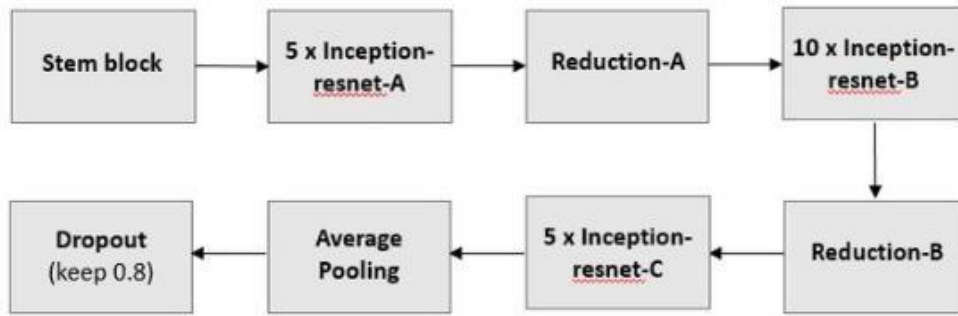


Figure 4. Basic network architecture of InceptionResnetV2

2.4. Model evaluation

For model evaluation, data were transmitted over the network and analysed with evaluation metrics such as overall accuracy, IoU, Dice similarity, precision, recall and F1-score. Confusion matrix table shows the actual and predicted values in a classification problem (Figure 5).

True positive (TP) and True negative (TN) are the areas where the model is correctly predicted, while False positive (FP) and False negative (FN) are the areas where the model is incorrectly predicted. Overall Accuracy is defined as the number of correctly classified pixels out of the total number of pixels (Equation 2).

$$OA = \frac{TP+TN}{TP+FP+TN+FN} \quad (2)$$

Since the overall accuracy is mainly influenced by the amount of unburned pixels due to the uneven distribution of classes, we calculated precision (Equation 3), which indicates how many of the values shown as positive are actually positive, and recall (Equation 4), which indicates how many of the pixels that we should have predicted as positive were able to predict as positive.

The harmonic mean of Precision and Recall values is used to calculate the F1-score. The reason for using the harmonic mean instead of a simple mean is that we should not ignore the extreme cases (Equation 5).

$$Precision = \frac{TP}{TP+FP} \quad (3)$$

$$Recall = \frac{TP}{TP+FN} \quad (4)$$

$$F_1 = 2 * \frac{precision * recall}{precision + recall} \quad (5)$$

In addition, IoU and Dice similarity coefficient metrics, also known as jaccard index, which are frequently used by artificial intelligence experts to measure the performance of segmentation models, were also calculated. IoU is defined as the similarity between ground truth and model prediction (Equation 6).

$$IoU = \frac{TP}{(TP+FP+FN)} \quad (6)$$

Similarly, another very reliable metric for analysing segmentation results is the Dice similarity coefficient (Equation 7).

$$DSC = \frac{2TP}{2TP+FP+FN} \quad (7)$$

In this study, the model was tested with data that it had not learnt before and was not entered into the training and its performance was evaluated with these metrics.

3. Results

The performance of the deep learning-based segmentation model (U-Net+InceptionResNetV2) was evaluated in the active fire detection and burnt area detection task. The related accuracy measurements were calculated on the test data set that was not learnt by the model during the training phase.

When training the CNN model, U-Net, an architecture consisting of encoder and decoder CNN layers, was used. Backbone is an architectural element that defines how these layers are organised in the encoder network and determines how the decoder network should be constructed. In this study, InceptionResNetV2 backbone, a CNN trained on more than one million images in the ImageNet database, is used. In the InceptionResNet block, multidimensional convolutional filters are combined with residual connections. The use of residual connections eliminates the distortion problem caused by deep structures and also reduces the training time (44).

In active fire detection using Sentinel 2 satellite images, high value pixels in SWIR bands (B12 and B11) and low value pixels in B4 band are filtered. B12, B11 and B4 bands are used in active fire detection. In burned area detection, the burned area in Sentinel 2 images causes a strong decrease in the near infrared (NIR) band (B8) and the resulting drought causes a moderate increase in the SWIR band (B12). Therefore, B12, B8 and B2 bands were used for burnt area detection. The final model was trained on the augmented data set using Red band and SWIR bands. In this study, the models were trained for an average of 4 hours each using Intel (R) Xeon (R) CPU @ 2.00 GHz, 8 cores, 64 Gb RAM and Tesla T4 GPU unit in the Colabratory environment provided by Google.

In each training epoch, training and validation data are passed over the network. In addition, IoU and loss values are calculated for both active fires (Figure 6) and burnt areas (Figure 7) in each epoch. IoU value, which is one of the most frequently used metrics in semantic segmentation, is calculated by dividing the overlap area between the predicted segmentation and the ground truth by the merging area between the predicted segmentation and the ground truth. This metric ranges from 0 to 1 (0 to 100 per cent), with 0 indicating no change and 1 indicating a perfectly overlapping segmentation. In the loss function, the system checks the error of its predictions and continuously tries to minimise the error. For this purpose, it calculates the error and tries to reduce it by means of an optimizer.

The evaluation results for the test patches are summarised in Table 2. In active fire detection with the U Net+InceptionResNetV2 model, a recall of 0.90, F1-score of 0.89, IoU of 0.82 and Dice score of 0.89 were obtained for 99 test images. In burnt area detection, a recall of

0.93, F1-score of 0.93, IoU of 0.88 and Dice score of 0.93 were obtained for 230 test images.

The results of three test patches from different regions are sampled (Figure 8). For active fires, the false color combination of the spectral bands B12, B11 and B4 is displayed, as well as the corresponding reference mask and the U-Net+InceptionResnetV2 estimate. Figure 9 shows an example of the results of four test patches from different regions for burnt areas. For burnt areas, the false colour combination of the B12, B8 and B2 spectral bands as well as the corresponding reference mask and the U-Net+InceptionResnetV2 estimate are displayed.

In order to test the study, two different regions with fire history given in Table 3 were analysed fully automatically.

The evaluation of the proposed automatic fire detection framework has been carried out with respect to detection accuracy and processing efficiency, visual quality control and location accuracy have been confirmed.

It was found that the fully automatic chain, controlled by optical satellite images obtained at any fire time by entering location and date information, reliably found small and fragmented burnt areas and active fires (Figure 10). In addition, the location information and area dimensions of the burnt areas of active fires are very important in terms of rapid intervention and subsequent revitalisation of the area. With this study, the mentioned information can be easily obtained automatically from the satellite image. Location and area information were determined separately for all active fires and burnt areas in the tested images. Table 4 shows an example of the location and area size data automatically determined by the software for both active fires and burnt areas.

4. Discussion

The selection of appropriate training data is the most important key point affecting the performance of the deep learning model. Considering this critical feature, not only patches containing both classes (burnt and clean area or active fire area and clean area), but also patches where one class is completely covered were used in the training of the models. Satellite images of many fires occurring in the world, which were pre-analysed visually, were used in the model training to facilitate the learning of artificial intelligence in the training phase.

Considering the IoU values (Table 2), which are evaluated in terms of the reliability of the model in segmentation studies in general, it is seen that the studies are quite successful, even small and fragmented active fires and burnt areas can be identified with high accuracy. Figure 6 and 7, which show the IoU and Loss values for the training and validation sets, it is seen that there are no problems such as overfitting and underfitting, and the graph oscillations are very good.

Test images taken from different parts of the world were analyzed with the relevant band combinations and reference masks were created. When these reference masks were compared with the model predictions, the success of the model was once again demonstrated (Figure 8 and 9).

In the study, when the active fire detection model and the burnt area detection model were evaluated within themselves, it was observed that the burnt areas had higher IoU values. This result is attributed to the fact that active fires are smaller and more fragmented and therefore have more background (i.e. clean area), whereas burnt areas are generally larger and more holistic. It was also observed that when testing the automated processing chain, agricultural areas and small volcanic rocks were rarely mixed with burnt areas.

However, in future studies, the success of the models can be improved by using more and various training data in both active fire detection and burnt area detection.

In spite of a few shortcomings mentioned above, which could be improved in the future, the proposed fully automated processing chain provides a product that can successfully identify active fires and burnt areas with high accuracy, in terms of geographical coordinates and fire size.

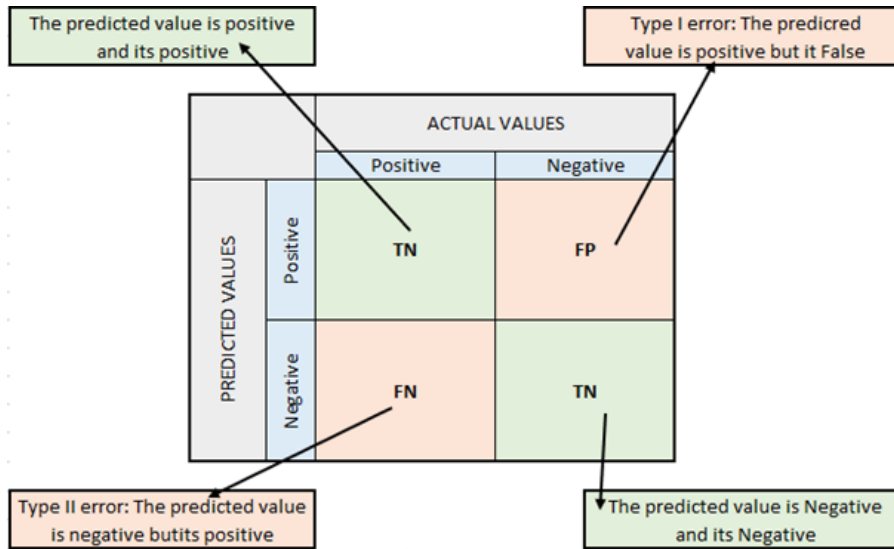


Figure 5. Confusion matrix

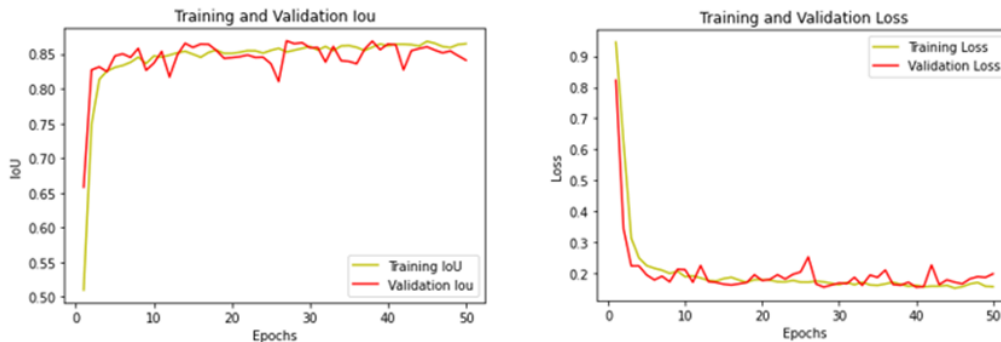


Figure 6. Training history of active fire detection model showing IoU and Loss value for training and validation dataset

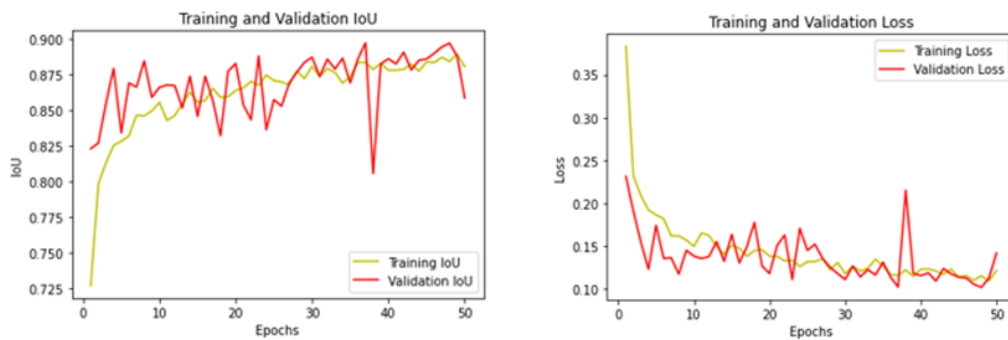


Figure 7. Training history of the burnt area detection model showing IoU and Loss value for the training and validation dataset

Table 2. Evaluation metrics for active fire and burnt area results of trained models

Detection	Overall Accuracy	Precision	Recall	F1- score	Dice Score	IoU
Active Fire	0.99	0.87	0.90	0.89	0.89	0.82
Burned Area	0.97	0.94	0.93	0.93	0.93	0.88

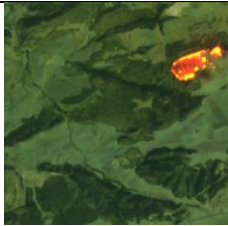



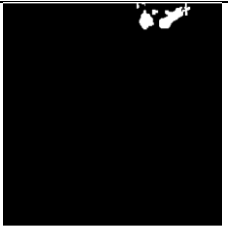

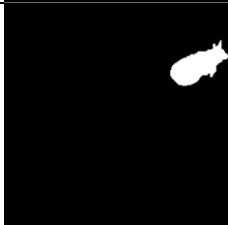
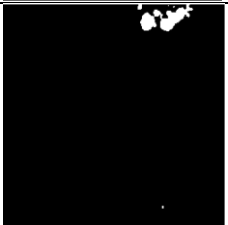
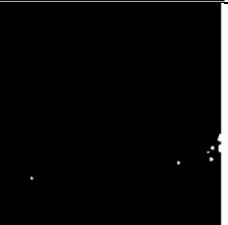
Test Area	Algeria	California	USA
False Color (B12, B11, B4)			
Reference Mask			
Model Prediction			

Figure 8. False color composition for spectral bands, reference mask and final model prediction of active fire (B12, B11 and B4) spectral bands for three different areas


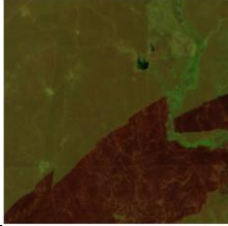






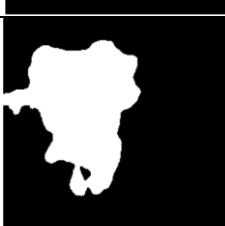
Test Area	Algeria 1	California	Algeria 2
False Color (B12, B8, B2)			
Reference Mask			
Model Prediction			

Figure 9. Reference mask and final model prediction of burned area (B12, B8 and B2) spectral bands for three different areas

Table 3. WGS 1984 UTM Zone 32N datum-based location information of optical satellite images used for test data

	Active Fire	Burned Area
Acquisition Date	2021-08-11	2021-08-12
Top	4103360	4103440
Left	396540	497220
Right	512840	613540
Bottom	3986980	3986900

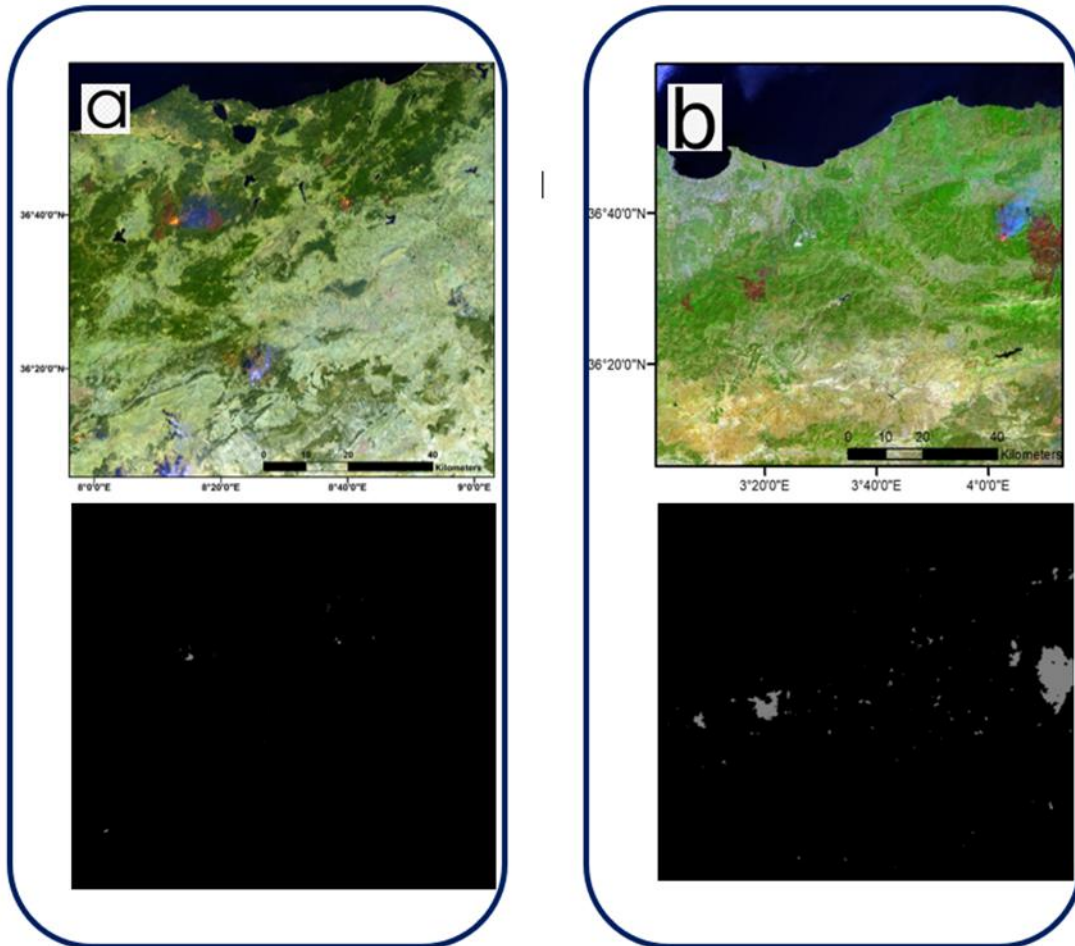


Figure 10. For the test area specified in Table 3; a) Active fire predict image, b) Burnt area predict image

Table 4. Example of automatically determined active fire and burned area zones and sizes (WGS 1984 UTM Zone 32N)

	Ymin	Ymax	Xmin	Xmax	Size (m ²)
Active Fire	4061940	4062860	468860	469420	11920
Burnt Area	4055620	4056360	605360	605820	13290

5. Conclusion

In this study, a fully automatic processing chain based on data collection, pre-processing and deep learning that can determine the location and size of active fires and burnt areas is presented for instant and reliable detection of active fires and rapid and reliable detection and rehabilitation of burnt areas. It is trained on the U-Net+InceptionResNetV2 model, which allows the analysis of active fires using SWIR2, NIR and Red bands of Sentinel 2 products and burnt areas using SWIR bands and blue band. The segmentation model is based on a deep neural network and achieved an overall accuracy of 0.99 and IoU of 0.82 for active fires and an overall accuracy of 0.97 and IoU of 0.88 for burnt areas. In addition, in the analysis performed with test data not

previously trained by the model, it was found to be very successful in finding small and fragmented fires and burnt areas.

Remote sensing satellites will be equipped with sensors with increasingly higher spatial and temporal resolution, enabling more precise and periodic monitoring. It is thought that the automatic processing chain presented in this study will be optimized in time and will provide great advantages in the rapid detection of active fires and in the revitalization of burnt areas.

Acknowledgement

The authors thank Copernicus for providing data for this study for scientific purposes.

Author contributions

Yasin Demirel: Literature research, Software Development, Analysis, Writing. **Tarik Türk:** Idea, Literature research, Analysis, Writing and Supervision.

Conflicts of interest

The authors declare no conflicts of interest.

Availability of data and materials

The data used within the scope of the study was obtained from <https://dataspace.copernicus.eu/>. The data generated/analyzed for this study are included in this article.

References

- Kavzoğlu, T. (2021). Orman yangınları sebepleri, etkileri, izlenmesi, alınması gereken önlemler ve rehabilitasyon faaliyetleri, Türkiye Bilimler Akademisi Yayınları
- Şeker, M. (2021). Orman yangınları sebepleri, etkileri, izlenmesi, alınması gereken önlemler ve rehabilitasyon faaliyetleri, Türkiye Bilimler Akademisi Yayınları
- Knopp, L., Wieland, M., Rättich, M., & Martinis, S. (2020). A deep learning approach for burned area segmentation with Sentinel-2 data. *Remote Sensing*, 12(15), 2422.
- Zhang, Q., Ge, L., Zhang, R., Metternicht, G. I., Liu, C., & Du, Z. (2021). Towards a deep-learning-based framework of Sentinel-2 imagery for automated active fire detection. *Remote Sensing*, 13(23), 4790.
- Nolde, M., Plank, S., & Riedlinger, T. (2020). An adaptive and extensible system for satellite-based, large scale burnt area monitoring in near-real time. *Remote Sensing*, 12(13), 2162
- Chuvieco, E., Mouillot, F., Van der Werf, G. R., San Miguel, J., Tanase, M., Koutsias, N., ... & Giglio, L. (2019). Historical background and current developments for mapping burned area from satellite Earth observation. *Remote Sensing of Environment*, 225, 45-64.
- Laris, P. S. (2005). Spatiotemporal problems with detecting and mapping mosaic fire regimes with coarse-resolution satellite data in savanna environments. *Remote sensing of environment*, 99(4), 412-424.
- Farhadi, H., Ebadi, H., & Kiani, A. (2023). Badi: a Novel Burned Area Detection Index for SENTINEL-2 Imagery Using Google Earth Engine Platform. *ISPRS Annals of the Photogrammetry, Remote Sensing and Spatial Information Sciences*, 10, 179-186.
- Pulvirenti, L., Squicciarino, G., Fiori, E., Negro, D., Gollini, A., & Puca, S. (2023). Near real-time generation of a country-level burned area database for Italy from Sentinel-2 data and active fire detections. *Remote Sensing Applications: Society and Environment*, 29, 100925.
- Gajardo, J., Mora, M., Valdés-Nicolao, G., & Carrasco-Benavides, M. (2022). Burned Area Classification Based on Extreme Learning Machine and Sentinel-2 Images. *Applied Sciences*, 12(1), 9.
- Kavzoğlu, T., Çölkesen, İ., Tonbul H. & Öztürk M., (2021). Uzaktan Algılama Teknolojileri ile Orman Yangınlarının Zamansal Analizi: 2021 Yılı Akdeniz ve Ege Yangınları, Türkiye Bilimler Akademisi Yayınları
- Musaoğlu, N., Yanalak M., Güngöroğlu C., Özcan O., (2021)., Orman yangınlarının yönetiminde bilgi teknolojilerinin katkıları, Türkiye Bilimler Akademisi Yayınları
- De Almeida Pereira, G. H., Fusioka, A. M., Nassu, B. T., & Minetto, R. (2021). Active fire detection in Landsat-8 imagery: A large-scale dataset and a deep-learning study. *ISPRS Journal of Photogrammetry and Remote Sensing*, 178, 171-186.
- Seydi, S. T., Saeidi, V., Kalantar, B., Ueda, N., & Halin, A. A. (2022). Fire-Net: A deep learning framework for active forest fire detection. *Journal of Sensors*, 2022, 1-14.
- Boothman, R., & Cardille, J. A. (2022). New techniques for old fires: Using deep learning to augment fire maps from the early satellite era. *Frontiers in Environmental Science*, 1253.
- Khryashchev, V., & Larionov, R. (2020, March). Wildfire segmentation on satellite images using deep learning. In *2020 Moscow Workshop on Electronic and Networking Technologies (MWENT)* (pp. 1-5). IEEE.
- Atasever, Ü. H., & Tercan, E. (2024). Deep learning-based burned forest areas mapping via Sentinel-2 imagery: a comparative study. *Environmental Science and Pollution Research*, 31(4), 5304-5318.
- Fusioka, A. M., Pereira, G. H., Nassu, B. T., & Minetto, R. (2024). Sentinel-2 Active Fire Segmentation: Analyzing Convolutional and Transformer Architectures, Knowledge Transfer, Fine-Tuning and Seam-Lines. *IEEE Geoscience and Remote Sensing Letters*.
- Escuin, S., Navarro, R., & Fernández, P. (2008). Fire severity assessment by using NBR (Normalized Burn Ratio) and NDVI (Normalized Difference Vegetation Index) derived from LANDSAT TM/ETM images. *International Journal of Remote Sensing*, 29(4), 1053-1073.
- Trigg, S., & Flasse, S. (2001). An evaluation of different bi-spectral spaces for discriminating burned shrub-savannah. *International Journal of Remote Sensing*, 22(13), 2641-2647.
- Martín, M. P., Gómez, I., & Chuvieco, E. (2006). Burnt Area Index (BAIM) for burned area discrimination at regional scale using MODIS data. *Forest Ecology and Management*, (234), S221.
- Petropoulos, G. P., Kontoes, C., & Keramitsoglou, I. (2011). Burnt area delineation from a uni-temporal perspective based on Landsat TM imagery classification using Support Vector Machines. *International Journal of Applied Earth Observation and Geoinformation*, 13(1), 70-80.

23. Ramo, R., & Chuvieco, E. (2017). Developing a random forest algorithm for MODIS global burned area classification. *Remote Sensing*, 9(11), 1193.
24. Roy, D. P., Huang, H., Boschetti, L., Giglio, L., Yan, L., Zhang, H. H., & Li, Z. (2019). Landsat-8 and Sentinel-2 burned area mapping-A combined sensor multi-temporal change detection approach. *Remote Sensing of Environment*, 231, 111254.
25. Kartal M., & Polat Ö. (2022). Detection of benign and malignant skin cancer from dermoscopic images using modified deep residual learning model. *AITA Journal*, vol. 2, no. 2, pp. 10-18, 2022
26. Gürkahraman, K., & Karakiş, R. (2021). Brain tumors classification with deep learning using data augmentation. *Journal of the Faculty of Engineering and Architecture of Gazi University*, 36(2), 997-1011.
27. Maggiori, E., Tarabalka, Y., Charpiat, G., & Alliez, P. (2016). Convolutional neural networks for large-scale remote-sensing image classification. *IEEE Transactions on geoscience and remote sensing*, 55(2), 645-657.
28. Wieland, M., Li, Y., & Martinis, S. (2019). Multi-sensor cloud and cloud shadow segmentation with a convolutional neural network. *Remote Sensing of Environment*, 230, 111203.
29. Wurm, M., Stark, T., Zhu, X. X., Weigand, M., & Taubenböck, H. (2019). Semantic segmentation of slums in satellite images using transfer learning on fully convolutional neural networks. *ISPRS journal of photogrammetry and remote sensing*, 150, 59-69.
30. Wieland, M., & Martinis, S. (2019). A modular processing chain for automated flood monitoring from multi-spectral satellite data. *Remote Sensing*, 11(19), 2330.
31. [31] Luus, F. P., Salmon, B. P., Van den Bergh, F., & Maharaj, B. T. J. (2015). Multiview deep learning for land-use classification. *IEEE Geoscience and Remote Sensing Letters*, 12(12), 2448-2452.
32. M Rustowicz, R., Cheong, R., Wang, L., Ermon, S., Burke, M., & Lobell, D. (2019). Semantic segmentation of crop type in Africa: A novel dataset and analysis of deep learning methods. In *Proceedings of the IEEE/CVF Conference on Computer Vision and Pattern Recognition Workshops* (pp. 75-82).
33. Varul, Y. E., Adiyaman, H., Bakırman, T., Bayram, B., Alkan, E., Karaca, S. Z., & Topaloğlu, R. H. (2023). Preserving human privacy in real estate listing applications by deep learning methods. *Mersin Photogrammetry Journal*, 5(1), 10-17
34. M Rustowicz, R., Cheong, R., Wang, L., Ermon, S., Burke, M., & Lobell, D. (2019). Semantic segmentation of crop type in Africa: A novel dataset and analysis of deep learning methods. In *Proceedings of the IEEE/CVF Conference on Computer Vision and Pattern Recognition Workshops* (pp. 75-82).
35. Körez, A. (2020). Derin öğrenme kullanarak uzaktan algılama görüntülerindeki nesnelere tespiti, Gazi Üniversitesi
36. Hnatushenko, V., Hnatushenko, V., Kashtan, V. (2023a). Detection of Forest Fire Consequences on Satellite Images using a Neural Network. 43. *WissenschaftlichTechnische Jahrestagung der DGPF*, 31, 29-36.
37. Perez, L., Wang, J., 2017. The effectiveness of data augmentation in image classification using deep learning. *arXiv preprint arXiv:1712.04621*.
38. Shijie, J., Ping, W., Peiyi, J., Siping, H., 2017. Research on data augmentation for image classification based on convolution neural networks. 2017 Chinese automation congress (CAC), IEEE, 4165-4170.
39. Hnatushenko, V., Soldatenko, D., & Heipke, C. (2023b). Enhancing the quality of CNN-based burned area detection in satellite imagery through data augmentation. *International Archives of the Photogrammetry, Remote Sensing and Spatial Information Sciences (ISPRS Archives)*; XLVIII-1/W2-2023, 48, 1749-1755.
40. Tran, T., Pham, T., Carneiro, G., Palmer, L., Reid, I., 2017. A bayesian data augmentation approach for learning deep models. *Advances in neural information processing systems*, 30.
41. Hnatushenko, V., Zhernovyi, V. (2020). Method of improving instance segmentation for very high resolution remote sensing imagery using deep learning. *Data Stream Mining & Processing: Third International Conference, DSMP 2020, Lviv, Ukraine, August 21-25, 2020, Proceedings 3*, Springer, 323-333.
42. Url-1: <https://keras.io/>, erişim tarihi:01.03.2023
43. Url-2: <https://scihub.copernicus.eu/dhus/#/home>, erişim tarihi:01.03.2023
44. Szegedy, C., Vanhoucke, V., Ioffe, S., Shlens, J., & Wojna, Z. (2016). Rethinking the inception architecture for computer vision. In *Proceedings of the IEEE conference on computer vision and pattern recognition* (pp. 2818-2826).
45. Kingma, D. P. (2014). Adam: A method for stochastic optimization. *arXiv preprint arXiv:1412.6980*.

